BIOCHEMISTRY
including biophysical chemistry & molecular biology
Article

Biochemistry **2009,** *48,* 9775–9784 9775
DOI: 10.1021/bi900634e

Novel Binding Motif of ACTH Analogues at the Melanocortin Receptors†

Yingkui Yang,*,‡ Victor J. Hruby,‖ Min Chen,§ Chiquito Crasto,§ Minying Cai,‖ and Carroll M. Harmon‡

‡*Department of Surgery and* §*Department of Genetics, University of Alabama, Birmingham, Alabama 35233, and* ‖*Department of Chemistry, University of Arizona, Tucson, Arizona 85721*

Received April 13, 2009; Revised Manuscript Received September 8, 2009

ABSTRACT: The melanocortin receptor (MCR) subtype family is a member of the GPCR superfamily, and each of them has a different pharmacological profile with regard to the relative potency of the endogenous and synthetic melanocortin peptides. α-MSH and ACTH are endogenous nonselective agonists for MC1R, MC3R, MC4R, and MC5R. In this study, we examined the role of Phe^7 in ACTH on human (h) MC1R, MC3R, and MC4R binding and signaling. Our results indicate that substitution of Phe^7 with D-$Nal(2')^7$ in ACTH1−24 yields a pharmacological profile different from that for substitution of Phe^7 with D-$Nal(2')^7$ in MSH in hMC1R, hMC3R, and hMC4R. N-D-$Nal(2')^7$-ACTH1−24 is an agonist at hMC3R and hMC4R which did not change the peptide from an agonist to an antagonist at hMC3R and hMC4R. Further experiments indicate that N-D-$Nal(2')^7$-ACTH1−17 is the minimal peptide required for hMC3R and hMC4R activation. Single-amino acid substitution studies of D-$Nal(2')^7$-ACTH1−17 indicate that amino acid residues 15−17 in N-D-$Nal(2')^7$-ACTH1−17 are crucial for hMC3R and hMC4R activation. Substitutions of these amino acid residues reduced or abolished agonist activity at hMC3R and hMC4R. Conformational studies revealed a new β-turn (Arg^8-Trp^9-Gly^{10}-Lys^{11}) in N-D-$Nal(2')^7$-ACTH1−17, compared to the β-turn-like structure at NDP-α-MSH (His^6-D-Phe^7-Arg^8-Trp^9). Our results suggest that NDP-α-MSH and N-D-$Nal(2')^7$-ACTH1−17 do not share the same binding site; the highly basic C-terminal fragment (Lys^{15}-Lys^{16}-Arg^{17}) of N-D-$Nal(2')^7$-ACTH1−17 induced a new β-turn, and this shift contributed the selective agonist activity at hMC3R and hMC4R.

The five known subtypes of human melanocortin receptors (hMC1−5R) are members of the superfamily of seven-transmembrane G-protein-coupled receptors (GPCRs)[1] expressed in various tissues, including in the skin (hMC1R) (*1*, *2*), in the adrenal cortex (hMC2R) (*3*, *4*), and throughout the central nervous system (hMC3R, hMC4R, and hMC5R) (*5*). The melanocortin system has received much attention in recent years because of its involvement in a large number of important physiological functions, such as skin pigmentation (*1*, *2*), control of the immune system, erectile function (*6*), blood pressure and heart rate, control of feeding behavior and energy homeostasis (*7*, *8*), modulation of aggressive and defensive behavior, and mediation of pain (*9*−*12*). The endogenous melanocortin agonists include α-, β-, and γ-melanocyte-stimulating hormones (MSH) and adrenocorticotropin (ACTH), while Agouti signaling protein and Agouti-related protein have been identified as the endogenous antagonists (*13*, *14*).

Considerable effort has been directed toward the development of highly potent hMC3R, hMC4R-selective agonists, and antagonists because of the involvement of these receptors in the regulation of feeding and sexual behavior (*15*−*23*). Most of the design work and the structure−activity relationship (SAR) work are based on MSH and its analogue. Almost all of the peptide agonists possess a β-turn-like structure in their binding pharmacophore (*24*−*28*). Comparatively little attention has been paid to ACTH, because of the dearth of specific evidence of their physiological functions in the melanocortin system and its larger size not being appropriate for drug development. Nevertheless, ACTH is active at hMCRs, and its structure information about the pharmacophore will be able to lead to drug design and selective cell signaling. Earlier reports have demonstrated that ACTH stimulation of MC2Rs in the adrenal cortex, especially in the zona fasciculate, results in the secretion of the glucocorticoids cortisol and corticoserone (*29*). Lately, it has been reported that ACTH plays an important physiological role in stimulating the fetal immune response which will be important for the study of cancer.

Several approaches to the design of hMC3R-selective agonists and antagonists have been described in the literature. Among the natural melanocyte-stimulating hormones, γ-MSH exhibits substantial hMC3R selectivity, whereas α-MSH and β-MSH exhibit little selectivity for any specific receptor subtype (*30*, *31*). A D-amino acid scan of the γ-MSH sequence revealed the importance of position 8 in hMC3R selectivity and led to the discovery of a highly selective hMC3R agonist (*30*). A D-Nal(2′) scan of linear α-MSH let to the discovery of a potent hMC3R/hMC5R antagonist and hMC4R agonist H-Tyr-Val-Nle-Gly-His-D-Nal(2′)-Arg-Trp-Asp-Arg-Phe-Gly-NH_2 (PB-II-94) (*32*). Structure−activity relationships of γ-MSH have yielded linear peptide analogues with enhanced potency and selectivity, most notably, the

†This work has been funded by National Institutes of Health Grants R03 HD047312-01A1 (Y.Y.) and DA 348900 and DA 06248 (V.J.H.).

*To whom correspondence should be addressed: Division of Pediatric Surgery, University of Alabama at Birmingham, 300 ACC, 1600 7th Ave., South Birmingham, AL 35233. Phone: (205) 939-9688. Fax: (205) 975-4972. E-mail: ying-kui.yang@ccc.uab.edu.

[1]Abbreviations: MCR, melanocortin receptor; GPCR, G-protein-coupled receptor; ACTH, adrenocorticotropic hormone; N-ACTH, Nle^4-adrenocorticotropic hormone; α-MSH, α-melanocyte-stimulating hormone; ASIP, Agouti signaling protein; TM, transmembrane domain; IBMX, 3-isobutylmethylxanthine; PCR, polymerase chain reaction; FACs, flow cytometry.

Published on Web 09/10/2009

nonselective superagonist Ac-Tyr-Val-Nle-Gly-His-D-Phe-Arg-Trp-Asp-Arg-Phe-Gly-NH_2 (Ac-NDP-γ-MSH-NH_2) (*31*), and recently, Hruby's laboratory has produced several potent and selective hMC3R agonists and hMC3R/hMC5R antagonists by placing a bulky hydrophobic Nle residue next to the melanocortin pharmacophore Xaa-Phe-Arg-Trp in a cyclic γ-MSH-derived template (*33*). Some cyclic α-MSH templates in which increased selectivity in hMC3R agonists and antagonists was observed have also been described. Thus, Kavarana et al. (*34*) have found that enhancing the hydrophobic properties of the cyclic α-MSH analogues and increasing the peptide macrocycle size resulted in improved hMC3R selectivity. Furthermore, Grieco et al. (*24*, *35*) have shown that certain dihedrally constrained amino acid substitutions at position 6 of Ac-Nle^4-c[Asp^5,D-Nal(2′)^7, Lys^{10}]α-MSH(4−10)-NH_2 (SHU9119) led to potent and highly hMC3R- and hMC4R-selective antagonists. Balse-Srinivasan et al. (*36*) have reported a series of cyclic disulfide α-MSH/β-MSH hybrid peptides with highly selective hMC3R {Ac-c[Pen-Glu-His-D-Nal(2′)-Arg-Trp-Cys]-Pro-Pro-Lys-Asp-NH_2} and hMC5R (Ac-c[Cys-Glu-His-D-Phe-Arg-Trp-D-Cys]-Pro-Pro-Lys-Asp-NH_2) antagonists.

The novel drug discovery study is based not only on the ligand structure information but also on the receptor structure information. The melanocortin receptors consist of a single polypeptide featuring seven α-helical transmembrane domains (TMs), an extracellular N-terminus, three extracellular loops, three intracellular loops, and an intracellular C-terminus. Many structural features conserved in other G-protein-coupled receptors are found in the melanocortin receptors (*37*, *38*). However, the melanocortin receptors lack several features found in most G-protein-coupled receptors: one or two cysteine residues in the first and second extracellular loops and proline found in the fourth and fifth TMs. This receptor structural information will be critical for finding the residues or domains that contribute to the selectivity of melanocortin system. Extensive studies have been performed using receptors chimeras with multiple-site-directed mutagenesis (*16*, *39*−*44*). In this study, we describe a series of ACTH analogues possessing a D-Nal(2′)^7 residue that have been designed to further pursue SAR trends leading to hMC3R and hMC4R agonist selectivity from both ligand structure and receptor structure studies.

EXPERIMENTAL PROCEDURES

Materials. All MSH and ACTH peptides were made by Genscript Inc. (Piscataway, NJ). To prevent oxidization, in all of the ACTHs the Met residues in position 4 were replaced with norleucine. The peptide sequence is given in Table 1. 3-Isobutylmethylxanthine (IBMX) was from Sigma, and [^{125}I]NDP-α-MSH was from Perkin-Elmer Life Sciences (Boston, MA). The HEK-293 cell line was purchased from ATCC (Manassas, VA), and DMEM and lipofectamine were from Life Technologies (Rockville, MD).

Site-Directed Mutagenesis of Human Melanocortin Receptors. A single mutation was constructed using the Quick-Change site-directed mutagenesis kit (Stratagene, La Jolla, CA). The entire coding region of the mutated receptors was sequenced to confirm that the desired mutation sequences were present and that no sequence errors had been introduced by the University of Alabama at Birmingham Sequence Core. The mutant receptors were then subcloned into eukaryotic expression vector pCDNA 3.1 (Invitrogen, Carlsbad, CA).

Cell Culture and Transfection. The HEK-293 cell line was utilized in this study. The cells were cultured in DMEM containing 10% bovine fetal serum and HEPES. Cells at 80% confluence were washed twice, and the receptor constructs were transfected into cells using lipofectamine (Life Technologies). The permanently transfected clonal cell lines were selected by resistance to the neomycin analogue G418.

Binding Assays. Binding experiments were performed using the conditions previously described (*16*). Briefly, after removal of the media, cells were incubated with nonradioligand at concentrations from 10^{-10} to 10^{-6} M in 0.5 mL of MEM containing 0.2% BSA and 2×10^5 cpm of [^{125}I]NDP-α-MSH for 1 h. We terminated the binding reactions by removing the medium and washing the cells twice with MEM containing 0.2% BSA. The cells were then lysed with 0.2 N NaOH, and the radioactivity in the lysate was quantified in an analytical gamma counter (PerkinElmer, Shelton, CT). Nonspecific binding was determined by measuring the amount of ^{125}I label bound on the cells in the presence of excess 10^{-6} M unlabeled ligand. We calculated specific binding by subtracting nonspecifically bound radioactivity from total bound radioactivity. Binding data are reported as IC_{50} values. K_i values for ligands were calculated using the equation $K_i = K_d = IC_{50} - [\text{radioligand}]$ (*45*).

cAMP Assay. Cellular cAMP generation was assessed using a competitive binding assay kit (TRK 432, Amersham, Arlington Heights, IL). Briefly, cell culture medium was removed, and cells were incubated with 0.5 mL of Earle's Balanced Salt Solution (EBSS), containing the melanocortin agonist (10^{-10}−10^{-6} M), for 1 h at 37 °C in the presence of 10^{-3} M isobutylmethylxanthine. The reaction was stopped by addition of ice-cold 100% ethanol (500 μL/well). The cells in each well were scraped, transferred to a 1.5 mL tube, and centrifuged for 10 min at 1900*g*, and the supernatant was evaporated in a 55 °C water bath with prepurified nitrogen gas. cAMP content was measured as previously described, according to instructions accompanying the assay kit (*46*).

Receptor Expression Using FACs. To determine whether the receptor proteins are expressed at the cell surface, we generated a chimeric hMC4R with the N-terminal fusion to the FLAG protein (Flag-hMC4R). The FLAG protein is an eight-amino acid peptide (Asp-Tyr-Lys-Asp-Asp-Asp-Asp-Lys), and FLAG-tagged receptor expression vectors have been widely used to purify receptor protein and to assess protein expression (*47*). Cells transfected with the receptors were harvested using 0.2% EDTA and washed twice with phosphate-buffered saline (PBS). Aliquots of 3×10^6 cells were centrifuged and fixed with 3% paraformaldehyde in PBS (pH 7.4). The cells were incubated with 50 μL of 10 μg/mL murine anti-FLAG M1 monoclonal antibody (Sigma, catalog no. 316) in incubation buffer for 45 min. Under this condition, the primary antibody binds only to receptors located on the cell surface. The cells were collected by centrifugation and washed three times with incubation buffer. The cell pellets were suspended in 100 μL of incubation buffer containing CY3-conjugated affinity pure donkey anti-mouse IgG (ImmunoResearch Lab, Inc., West Grove, PA) and incubated at room temperature for 30 min. Flow cytometry was performed on a fluorescence-activated cell sorter (FACStar plus six-parameter cytometer/sorter with a dual argon ion laser, Becton Dickinson, San Jose, CA). The results were analyzed using CellQuest (Beckton-Dickinson Immunocytometry Systems, San Jose, CA).

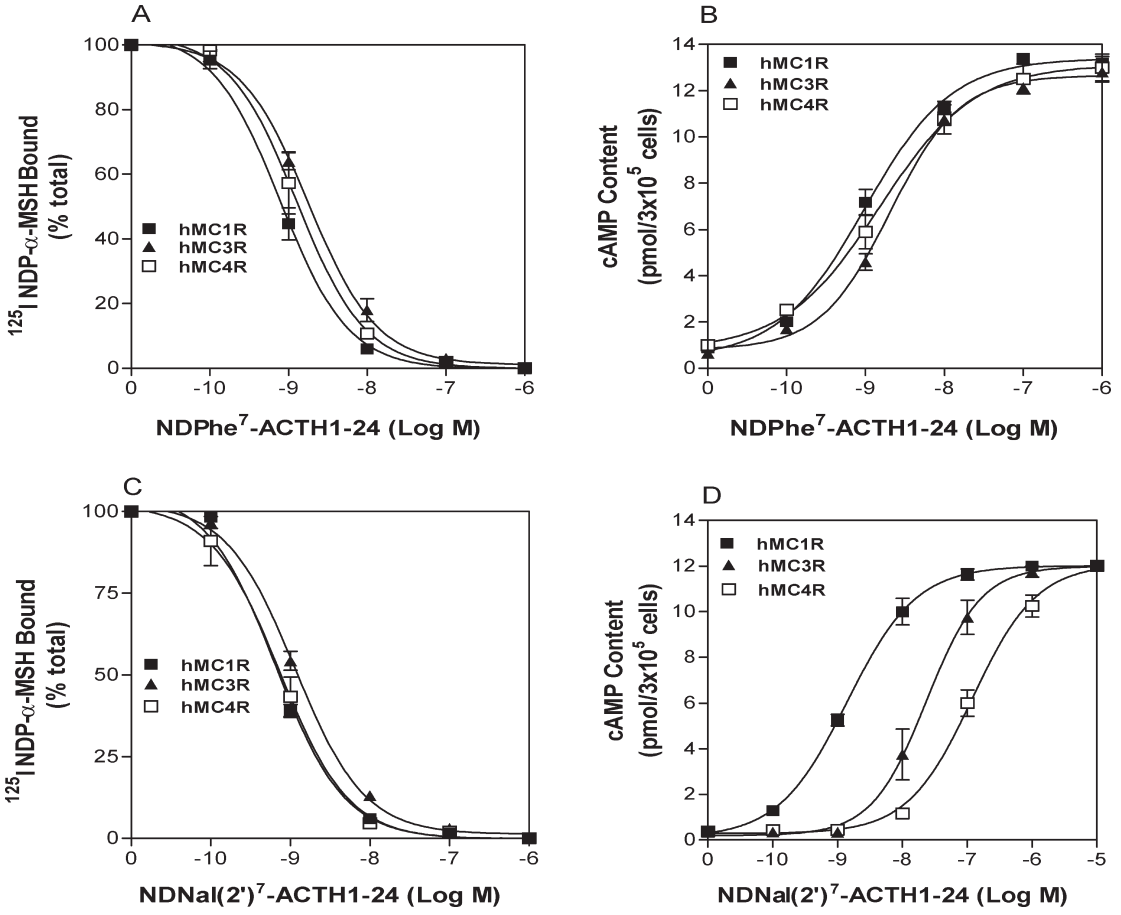

FIGURE 1: Binding affinity and potency of NDP-α-MSH and ACTH(1−24) analogues at wild-type hMC1R, hMC3R, and hMC4R. Panels A and C show the effect of the ACTH analogue on [^{125}I]ACTH binding at hMC1R, hMC3R, and hMC4R. Panels B and D show the effect of the ACTH analogue on total cAMP accumulation at hMC1R, hMC3R, and hMC4R ($n \geq 3$) (see Table 2 for K_i and EC_{50} values).

Computational Procedures. Molecular modeling experiments employed MacroModel version 9.1 equipped with Maestro 7.5 graphical interface (Schrödinger, LLC, New York, NY) installed on a Linux Red Hat 9.0 system and were performed as previously described (*33*). Peptide structures were built into extended structures with standard bond lengths and angles, and they were minimized using the OPLS 2005 force field and the Polak-Ribier conjugate gradient (PRCG). Optimizations were converged to a gradient root-mean-square deviation of < 0.05 kJ Å^{-1} mol^{-1} or continued until a limit of 50000 iterations was reached. Aqueous solution conditions were simulated using the continuum dielectric water solvent model (GB/SA). Extended cutoff distances were defined: 8 Å for van der Waals, 20 Å for electrostatics, and 4 Å for H-bonds.

Conformational profiles of the peptides were investigated by the hybrid Monte Carlo/Low Frequency Mode (MCMM/LMCS) (*48*) procedure as implemented in Macromodel using the energy minimization parameters as described above. MCMM torsional variations and Low Mode parameters were set up automatically within the Maestro graphical user interface. A total of 20000 search steps were performed, and the conformations with an energy difference from the global minimum of 50 kJ/mol were saved. Interatomic dihedral angles were measured for each peptide analogue using the Maestro graphical user interface, and they are listed in Table 4.

Statistical Analysis. Each experiment was performed in duplicate three separate times. The mean value of the dose−response data of binding and cAMP production was fitted to a sigmoidal curve with a variable slope factor using nonlinear squares regression analysis (Graphpad Prism, Graphpad Software, San Diego, CA). Data are expressed as means ± the standard error of the mean. Statistical significance was assessed by one-way ANOVA ($P < 0.05$).

RESULTS

D-Phe^7- and D-Nal(2')^7-ACTH Analogue Binding and Activity. It is well-known that the amino acid Phe^7 in MSH is critical for agonist activity at MC3R and MC4R. Substitution of Phe^7 in MSH with D-Phe^7 results in an increase in agonist activity, but replacement of D-Phe^7 with D-Nal(2')^7 caused the ligand to lose agonist activity at MC3R and MC4R (*28*). To determine whether Phe^7 in ACTH is also crucial for hMC3R and hMC4R binding and activation, we examined the substitutions of D-Phe^7 in ACTH on receptor binding. N-D-Phe^7-ACTH dose-dependently displaces [^{125}I]NDP-α-MSH binding at hMC3R and hMC4R (Figure 1A). The binding affinities of N-D-Phe^7-ACTH analogues are higher than that of NPhe^7-ACTH analogues. Consistent with binding data, N-D-Phe^7-ACTH dose-dependently increased the level of cAMP generation at hMC3R and hMC4R (Figure 1B). N-D-Phe^7-ACTH has a high agonist potency compared to that of NPhe^7-ACTH. The role of D-Phe^7 in ACTH is similar to that of NDP-α-MSH, and their IC_{50} and EC_{50} values are listed in Table 2.

To determine whether D-Nal(2')^7 in ACTH is also crucial for hMC3R and hMC4R activation, N-D-Nal(2')^7-ACTH was synthesized and tested. Our results indicate that N-D-Nal(2')^7-ACTH1−24

Table 1: Sequences of the Substituted ACTH Peptides

NDP-α-MSH	Ac-Ser-Tyr-Ser-**Nle**-Glu-His-**D-Phe**-Arg-Trp-Gly-Lys-Pro-Val-NH_2
N-D-Nal(2′)^7-α-MSH	Ac-Ser-Tyr-Ser-**Nle**-Glu-His-**D-Nal(2′)**-Arg-Trp-Gly-Lys-Pro-Val-Gly-NH_2
N-D-Phe^7-ACTH1−24	Ac-Ser-Tyr-Ser-**Nle**-Glu-His-**D-Phe**-Arg-Trp-Gly-Lys-Pro-Val-Gly-Lys-Lys-Arg-AA18−24-NH_2
N-D-Nal(2′)^7-ACTH1−24	Ac-Ser-Tyr-Ser-**Nle**-Glu-His-**D-Nal(2′)**-Arg-Trp-Gly-Lys-Pro-Val-Gly-Lys-Lys-Arg-AA18−24-NH_2
N-CTH1−17	Ac-Ser-Tyr-Ser-**Nle**-Glu-His-**Phe**-Arg-Trp-Gly-Lys-Pro-Val-Gly-Lys-Lys-Arg-NH_2
N-D-Nal(2′)^7-ACTH1−17	Ac-Ser-Tyr-Ser-**Nle**-Glu-His-**D-Nal(2′)**-Arg-Trp-Gly-Lys-Pro-Val-Gly-Lys-Lys-Arg-NH_2
N-D-Nal(2′)^7-ACTH1−14	Ac-Ser-Tyr-Ser-**Nle**-Glu-His-**D-Nal(2′)**-Arg-Trp-Gly-Lys-Pro-Val-Gly-NH_2
N-D-Nal(2′)^7-ACTH1−15	Ac-Ser-Tyr-Ser-**Nle**-Glu-His-**D-Nal(2′)**-Arg-Trp-Gly-Lys-Pro-Val-Gly-Lys-NH_2
N-D-Nal(2′)^7-ACTH1−16	Ac-Ser-Tyr-Ser-**Nle**-Glu-His-**D-Nal(2′)**-Arg-Trp-Gly-Lys-Pro-Val-Gly-Lys-Lys-NH_2
N-D-Nal(2′)^7-Nle^{15}-ACTH1−17	Ac-Ser-Tyr-Ser-**Nle**-Glu-His-**D-Nal(2′)**-Arg-Trp-Gly-Lys-Pro-Val-Gly-**Nle**-Lys-Arg-NH_2
N-D-Nal(2′)^7-Nle^{16}-ACTH1−17	Ac-Ser-Tyr-Ser-**Nle**-Glu-His-**D-Nal(2′)**-Arg-Trp-Gly-Lys-Pro-Val-Gly-Lys-**Nle**-Arg-NH_2
N-D-Nal(2′)^7-Nle^{17}-ACTH1−17	Ac-Ser-Tyr-Ser-**Nle**-Glu-His-**D-Nal(2′)**-Arg-Trp-Gly-Lys-Pro-Val-Gly-Lys-Lys-**Nle**-NH_2
NAIa^7-ACTH1−17	Ac-Ser-Tyr-Ser-**Nle**-Glu-His-**Ala**-Arg-Trp-Gly-Lys-Pro-Val-Gly-Lys-Lys-Arg-NH_2
N-D-Nal(2′)^7-Ala^8-ACTH1 −17	Ac-Ser-Tyr-Ser-**Nle**-Glu-His-**D-Nal(2′)**-**Ala**-Trp-Gly-Lys-Pro-Val-Gly-Lys-Lys-Arg-NH_2
N-D-Nal(2′)^7-Ala^9-ACTH1 −17	Ac-Ser-Tyr-Ser-**Nle**-Glu-His-**D-Nal(2′)**-Arg-**Ala**-Gly-Lys-Pro-Val-Gly-Lys-Lys-Arg- NH_2
N-D-Nal(2′)^7-Ala^{7,8,9}-ACTH1−17	Ac-Ser-Tyr-Ser-**Nle**-Glu-His-**Ala-Ala-Ala**-Arg-Trp-Gly-Lys-Pro-Val-Gly-Lys-Lys-Arg-NH_2

Table 2: Binding Affinities and Potencies of NDP-α-MSH and ACTH Analogues at hMC1R, hMC3R, and hMC4R

	hMC1R		hMC3R		hMC4R	
	K_i (nM)	EC_{50} (nM)	K_i (nM)	EC_{50} (nM)	K_i (nM)	EC_{50} (nM)
NDP-α-MSH	0.4 ± 0.03	0.7 ± 0.1	3.5 ± 1.0	1.8 ± 0.1	2.1 ± 0.2	1.0 ± 0.3
N-D-Nal(2′)^7-α-MSH	1.2 ± 0.3	1.8 ± 0.5	5.5 ± 1.0	NA[a]	3.4 ± 0.3	NA[a]
N-D-Phe^7-ACTH1−24	0.5 ± 0.2	1.0 ± 0.2	6.1 ± 0.6	0.6 ± 0.1	3.9 ± 0.4	1.3 ± 0.2
N-D-Nal(2′)^7-ACTH1−24	0.8 ± 0.3	2.7 ± 0.5	5.9 ± 0.8	83 ± 15	3.8 ± 0.1	134 ± 32

[a]No activity (at 10^{-6} M).

dose-dependently displaced [^{125}I]ACTH binding at hMC3R and hMC4R (Figure 1C), and its K_i is given in Table 2. Surprisingly, our results indicate that N-D-Nal(2′)^7-ACTH1−24 remains an agonist at hMC3R and hMC4R. Unlike N-D-Nal(2′)^7-α-MSH, N-D-Nal(2′)^7-ACTH1−24 was able to induce cAMP production at hMC3R and hMC4R, although N-D-Nal(2′)-7-ACTH1−24 has significantly decreased potency (nearly 100-fold) compared to that of NDP-α-MSH at hMC3R and hMC4R (Figure 1D). It suggests that D-Nal(2′)^7-ACTH1−24 has different binding sites compared to that of D-Nal(2′)^7-α-MSH.

Truncated D-Nal(2′)^7-ACTH Analogue Binding and Activity. To further investigate the region of ACTH that is crucial for D-Nal(2′)^7-ACTH activity, several truncated D-Nal(2′)^7-ACTH analogues were synthesized and tested. The sequences of the tested peptides are listed in Table 1. Our results demonstrated that the activities of these analogues are different at these MCRs. N-D-Nal(2′)^7-ACTH1−17 is the shortest sequence that can activate hMC3R and hMC4R (Figure 2). If D-Nal(2′)^7-ACTH analogues have fewer than 17 amino acids, the truncated peptides lose their agonist activities at hMC3R and hMC4R. Their K_i and EC_{50} values are listed in Table 3.

Effect of Single-Amino Acid Substitution on D-Nal(2′)^7-ACTH1−17 Analogue Binding and Activity. The first 13 amino acid residues of ACTH are identical to those of α-MSH. D-Nal(2′)^7-ACTH1−17 has only four more amino acids than D-Nal(2′)^7-NDP-α-MSH. The fact that D-Nal(2′)^7-ACTH1−17 is an agonist at hMC3R and hMC4R implies that residues Lys^{15}, Lys^{16}, and Arg^{17} are important for D-Nal(2′)^7-ACTH1−17 agonist activity. To evaluate the roles of amino acids 15, 16, and 17 in D-Nal(2′)^7-ACTH1−17 on hMC3R and hMC4R activation, these residues were replaced with norleucine individually (Table 1), and the effects of these peptides on cAMP production at hMC3R and hMC4R were examined. As shown in Figure 3, our results indicate that one of the substitutions of residues 15, 16, and 17 in D-Nal(2′)^7-ACTH1−17 resulted in the loss of peptide agonist activity at hMC3R and hMC4R, implying that these residues are essential for D-Nal(2′)^7-ACTH1−17 activity.

Although these peptides lose agonist activities at hMC3R and hMC4R, whether they still possess antagonist activity at hMC3R and hMC4R is unknown. We examined the abilities of the peptides, N-D-Nal(2′)^7-Nle^{15}-ACTH1−17, N-D-Nal(2′)^7-Nle^{16}-ACTH1−17, and N-D-Nal(2′)^7-Nle^{17}-ACTH1−17, to inhibit NDP-α-MSH-stimulated cAMP generation at hMC3R and hMC4R. The cells expressing hMC3R or hMC4R were incubated with these peptides (10^{-7} M) and NDP-α-MSH (10^{-10}−10^{-6} M). cAMP assays were performed, and these peptide antagonist activities were determined. As shown in Figure 4, our results indicate that introduction of the peptides resulted in a right shift of the NDP-α-MSH-induced dose−response curve, suggesting that these peptides potently inhibit NDP-α-MSH-stimulated cAMP production at hMC3R and hMC4R.

To determine whether the "Phe-Arg-Trp" core sequence in N-D-Nal(2′)^7-ACTH is also important for hMC3R and hMC4R activation, the peptide residues, Phe^7, Arg^8, and Trp^9, in D-Nal(2′)^7-ACTH1−17 were individually or collectively substituted with alanine, and their activities were tested at hMC1R, hMC3R, and hMC4R. Our results show that NAla^7-ACTH1−17 has a potency similar to that of N-D-Nal(2′)^7-ACTH1−17, which indicates that Phe^7 is not the key residue for agonist activation at hMC3R and hMC4R, whereas N-D-Nal(2′)^7-Ala^8-ACTH1−17 and N-D-Nal(2′)^7-Ala^9-ACTH1−19 resulted in a loss of agonist activity at hMC3R and hMC4R (Figure 5), suggesting that the "Arg^8-Trp^9" residues are crucial for D-Nal(2′)^7-ACTH agonist activity at hMC1R, hMC3R, and hMC4R.

Molecular modeling data show that in the lowest-energy conformation of N-D-Nal(2′)^7-ACTH1−17, there is a β-turn-like structure (Arg^8-Trp^9-Gly^{10}-Lys^{11}) in N-D-Nal(2′)^7-ACTH

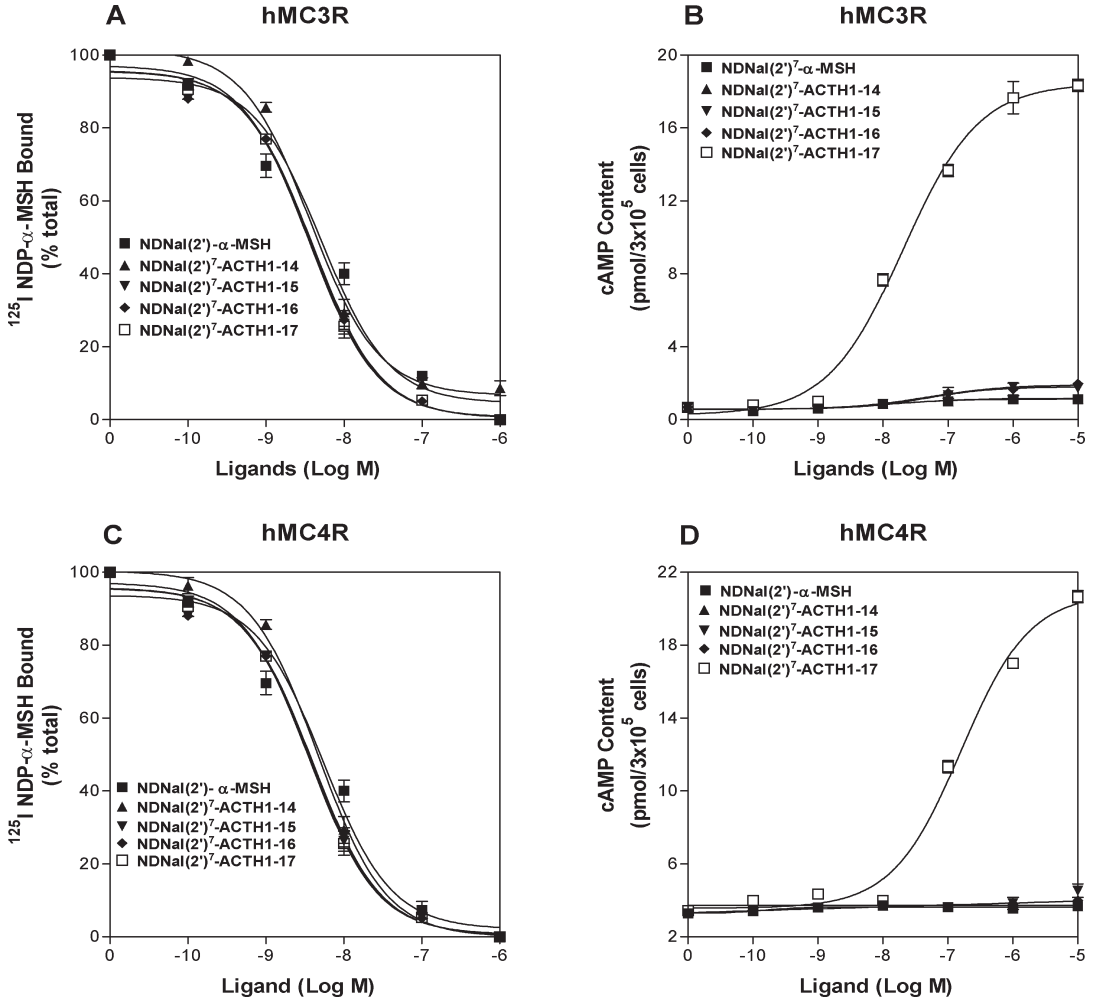

FIGURE 2: Binding affinity and potency of the truncated ACTH fragments at wild-type hMC3R and hMC4R. Panels A and C show the effects of the truncated ACTH fragments on [^{125}I]NDP-α-MSH binding at hMC3R and hMC4R. Panels B and D show the effects of the truncated ACTH fragments on total cAMP accumulation at hMC3R and hMC4R ($n \geq 3$) (see Table 3 for K_i and EC_{50} values).

Table 3: Affinities and Potencies of the Truncated ACTH Analogues at hMC1R, hMC3R, and hMC4R

	hMC1R		hMC3R		hMC4R	
	K_i (nM)	EC_{50} (nM)	K_i (nM)	EC_{50} (nM)	K_i (nM)	EC_{50} (nM)
N-D-Nal(2′)^7-α-MSH	0.92 ± 0.1	0.63 ± 0.03	5.3 ± 1.0	NA[a]	1.6 ± 0.3	NA[a]
N-D-Nal(2′)^7-Nle^4-ACTH 1−14	0.83 ± 0.2	0.671 ± 0.01	5.6 ± 0.9	NA[a]	1.8 ± 0.2	NA[a]
N-D-Nal(2′)^7-Nle^4-ACTH1−15	0.90 ± 0.2	0.71 ± 0.05	5.7 ± 1.5	NA[a]	1.3 ± 0.5	NA[a]
N-D-Nal(2′)^7-Nle^4-ACTH1−16	0.89 ± 0.16	0.65 ± 0.06	5.1 ± 1.6	NA[a]	1.8 ± 0.2	NA[a]
N-D-Nal(2′)^7-Nle^4-ACTH1−17	0.88 ± 0.17	0.58 ± 0.07	5.3 ± 1.1	95 ± 7	2.1 ± 0.6	184 ± 17
N-D-Nal(2′)^7-Nle^{15}-ACTH1−17	0.95 ± 0.13	0.5 ± 0.03	5.8 ± 0.8	NA[a]	1.4 ± 0.3	NA[a]
N-D-Nal(2′)^7-Nle^{16}-ACTH1−17	0.99 ± 0.15	0.45 ± 0.05	5.4 ± 1.4	NA[a]	1.5 ± 0.4	NA[a]
N-D-Nal(2′)^7-Nle^{17}-ACTH1−17	0.96 ± 0.13	0.56 ± 0.03	5.5 ± 0.9	NA[a]	1.7 ± 0.3	NA[a]
Ala^7-ACTH1−17	37.8 ± 5.2	7.8 ± 1.2	> 10^3	165 ± 15	> 10^3	257 ± 32
N-D-Nal(2′)^7-Ala^8-ACTH 1−17	10.9 ± 2.3	9.5 ± 3.0	> 10^3	293 ± 26	> 10^3	335 ± 27
N-D-Nal(2′)^7-Ala^9-ACTH 1−17	21.5 ± 4.7	16.5 ± 2.7	> 10^3	NA[a]	> 10^3	NA[a]
N-D-Nal(2′)^7-Ala^{7,8,9}-ACTH1−17	> 10^3	NA	> 10^3	NA[a]	> 10^3	NA[a]

[a]No activity (at 10^{-6} M).

(Figure 6). In this turn, Arg^8 and Trp^9 become the most important binding residues; Phe^7 is not involved the turn. Compared to the β-turn-like structure in NDP-α-MSH (His^6-D-Phe^7-Arg^8-Trp^9), the β-turn is shifted. This shift might contribute to the agonist activity at hMC3R and hMC4R for D-Nal(2′)^7-ACTH. Table 4 lists both the backbone dihedral angle conformation and side chain dihedral angle conformation.

Effects of Substitution of the TM3 Residue of hMC1R, hMC3R, and hMC4R on D-Nal(2′)-ACTH1−17 Activity. Transmembrane domain 3 of the melanocortin receptors has been identified as playing an important role in ligand selectivity for receptor activation. Residues L165 and L133 in TM3 of hMC3R and hMC4R have been identified as being crucial for SHU9119 selectivity. Substitutions of these residues of hMC3R

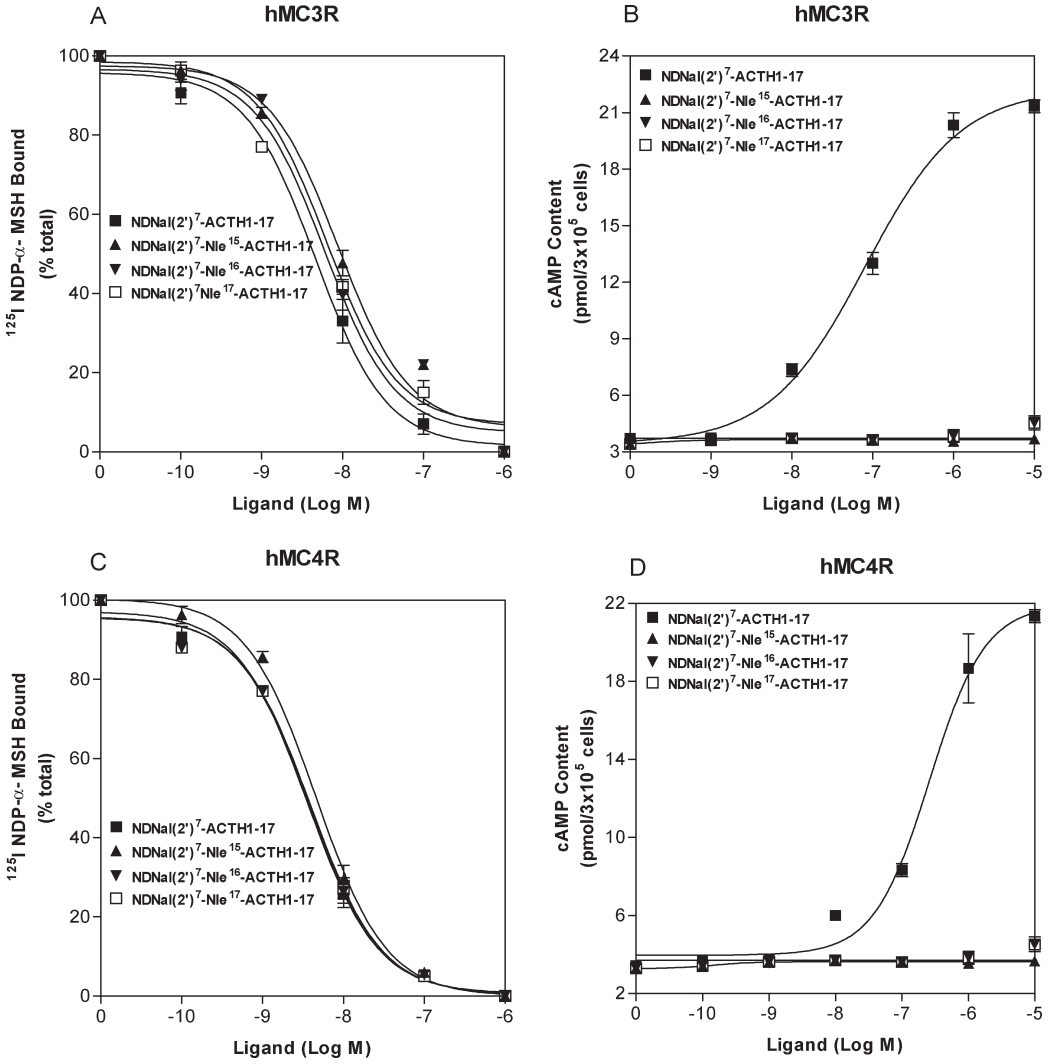

FIGURE 3: Binding affinity and potency of ACTH analogues at wild-type hMC3R and hMC4R. Panels A and C show the effects of the ACTH analogue on [^{125}I]NDP-α-MSH binding at hMC3R and hMC4R. Panels B and D show the effects of the ACTH analogue on total cAMP accumulation at hMC3R and hMC4R ($n \geq 3$) (see Table 3 for K_i and EC_{50} values).

and hMC4R with the corresponding region of hMC1R switched SHU9119 from an antagonist to an agonist (*42*). To determine whether these residues are also responsible for N-D-Nal(2′)^7-ACTH1−17 specific activities at hMC1R, hMC3R, and hMC4R, we tested this new compound on these previously made mutant receptors. We tested the L165M substitution of hMC3R and the L133M substitution of hMC4R and examined the effects of the mutations on N-D-Nal(2′)^7-ACTH1−17 agonist activity. As shown in Figure 7, our results indicate that L165M and L133M did not dramatically increase N-D-Nal(2′)^7-ACTH1−17 agonist potency, suggesting that these residues are not crucial for N-D-Nal(2′)^7-ACTH1−17 agonist activity. To determine whether the corresponding residue in hMC1R is also responsible for N-D-Nal(2′)^7-ACTH1−17 specific activity, we substituted amino acid residue M128 in TM3 of hMC1R with methione. Cells expressing M128L were treated with N-D-Nal(2′)^7-ACTH1−17. Ligand agonist potency was evaluated. Our results indicate that unlike the L156M and L133M substitutions in hMC3R and hMC4R, the M128L substitution did significantly decrease N-D-Nal(2′)^7-ACTH1−17 agonist potency, suggesting that this residue is crucial for N-D-Nal(2′)^7-ACTH1−17 activity (Table 5).

DISCUSSION

ACTH is an endogenous agonist for all MCRs. Its first 13 amino acid residues are identical to those of α-MSH. It is generally believed that ACTH shares a similar binding site with α-MSH at MC3R and MC4R. However, this study demonstrates that N-D-Nal(2′)^7-ACTH1−17 has different binding sites at hMC3R and hMC4R. N-D-Nal(2′)^7-ACTH1−17, which has four additional amino acid residues compared to N-D-Nal(2′)^7-α-MSH, is able to induce cAMP production at hMC3R and hMC4R, whereas N-D-Nal(2′)^7-α-MSH cannot. This implies that the four extra amino acids at the C-terminus of N-D-Nal(2′)^7-ACTH1−17 play an important role in agonist selectivity. Our further work supports this hypothesis. We found that substitution of amino acid residues Lys^{15}, Lys^{16}, and Arg^{17}, one at a time, of the peptide results in the loss of analogue agonist activity at hMC3R and hMC4R, proving that these residues are important for receptor activation. Adding four amino acid residues to N-D-Nal(2′)^7-α-MSH switches the peptide from an antagonist to an agonist, suggesting that N-D-Nal(2′)^7-ACTH1−17 may have different binding sites at hMC3R and hMC4R compared to NDP-α-MSH.

The intriguing biological results triggered further conformational studies. As mentioned earlier, SAR studies have found that

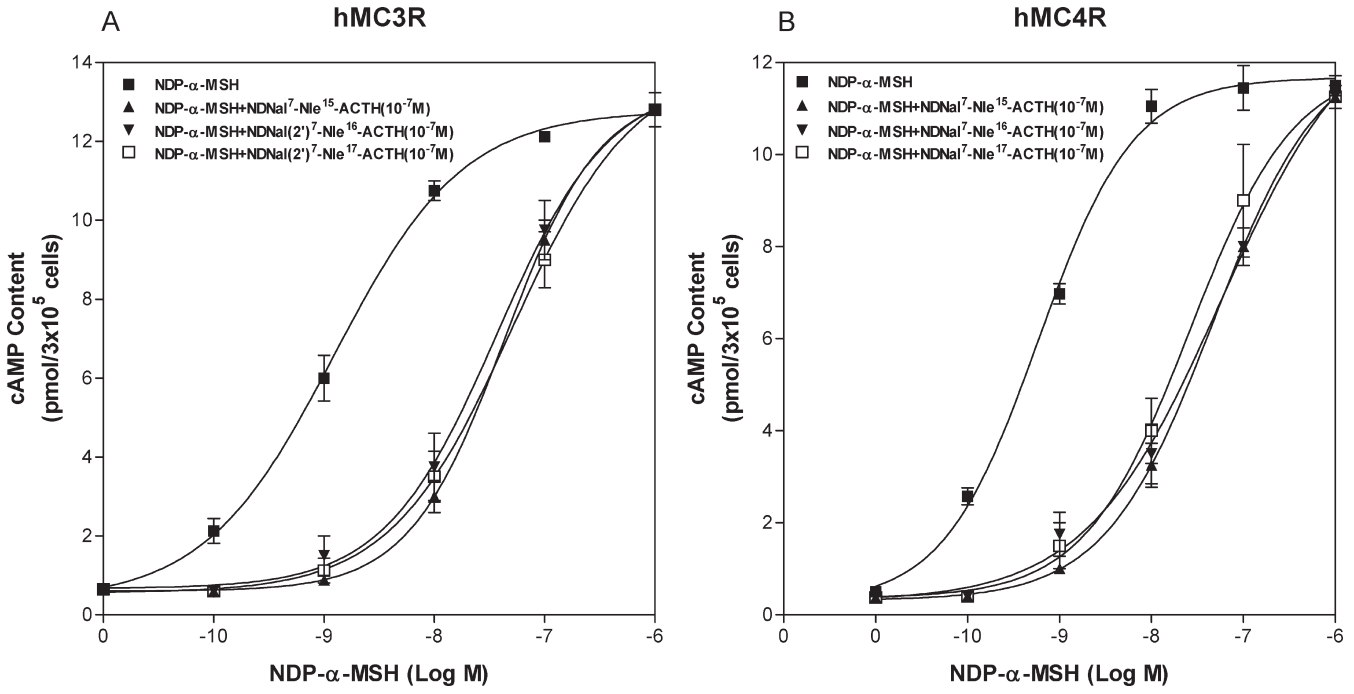

FIGURE 4: Effects of the mutated ACTH analogues on NDP-α-MSH-mediated cAMP production. (A) Effect of the mutated ACTH analogues on NDP-α-MSH-mediated cAMP production at hMC3R. (B) Effect of the mutated ACTH analogues on NDP-α-MSH-mediated cAMP production at hMC4R.

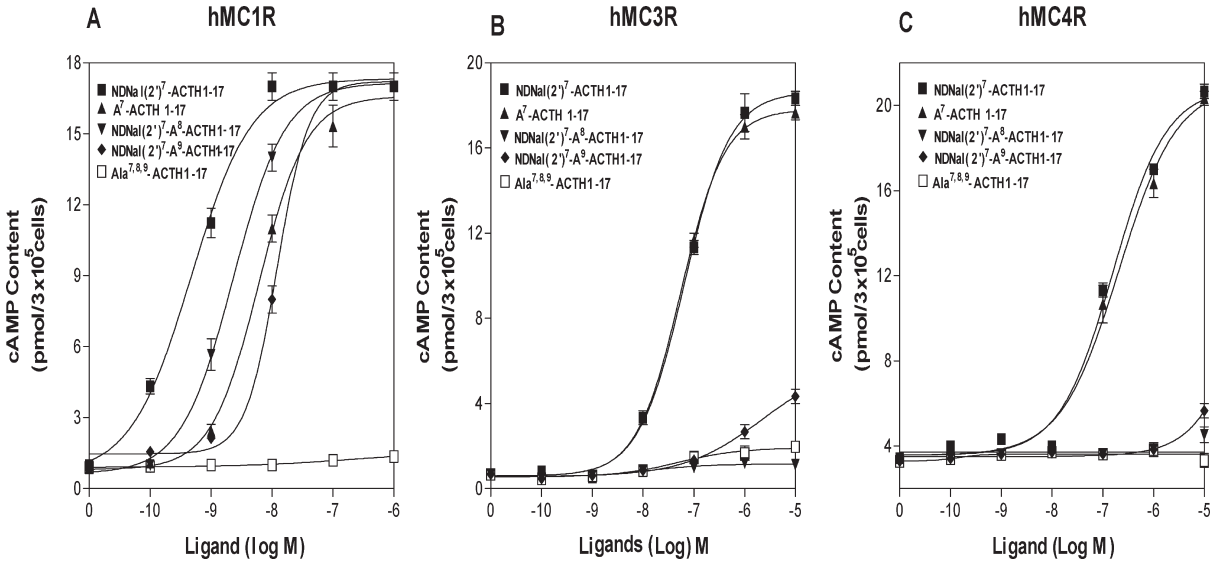

FIGURE 5: Binding affinities and potencies of ACTH analogues at wild-type hMC1R, hMC3R, and hMC4R. Panel A shows the effects of ACTH analogues on total cAMP accumulation at hMC1R. Panel B shows the effects of ACTH analogues on total cAMP accumulation at hMC3R. Panel C shows the effects of ACTH analogues on total cAMP accumulation at hMC4R ($n \geq 3$) (see Table 3 for K_i and EC_{50} values).

residue Phe^7 in α-MSH is responsible for MC3R and MC4R activation but not in the case of N-D-Nal^7-ACTH activation at MC3R and MC4R. The Arg^8-Trp^9 pair plays a critical role in N-D-Nal^7-ACTH activation at MC3R and MC4R. A global minimum search has been performed. The lowest-energy conformation of N-D-Nal^7-ACTH1−17 shows that there is a new β-turn-like structure at Arg^8-Trp^9-Gly^{10}-Lys^{11} (Figure 6). Compared to the β-turn-like structure of NDP-α-MSH (His^6-D-Phe^7-Arg^8-Trp^9), the new β-turn is shifted and Phe^7 is not involved in the new β-turn. Table 4 show the backbone torsion angles (degrees) for the global minima of selected N-D-Nal(2′)^7-ACTH1−17 forms. It is noted that D-Nal(2′)^7 is completely twisted 180° but Arg^8 and Trp^9 remain very close to the backbone conformation (Table 4). The biological data further prove that without Phe^7, NAla^7-ACTH1−17 is still an active potent agonist at hMC3R and hMC4R. Therefore, the new β-turn shift might be contribute to the agonist activity at hMC3R and hMC4R.

To further determine how the peptide forms the new β-turn, we analyzed the structure of N-D-Nal^7-ACTH1−17. The highly basic residues, Lys^{15}, Lys^{16}, and Arg^{17}, at the C-terminus of N-D-Nal(2′)^7-ACTH1−17 formed a few more hydrogen bonds and a very hydrophilic surface. This forced the β-turn to shift. Without these three residues, the β-turn will be His^6-D-Phe^7-Arg^8-Trp^9 like that of NDP-α-MSH. The mutation of these basic amino acids resulted in a dramatic loss of potency at hMC3R and hMC4R. Therefore, strong electrostatic residues at the

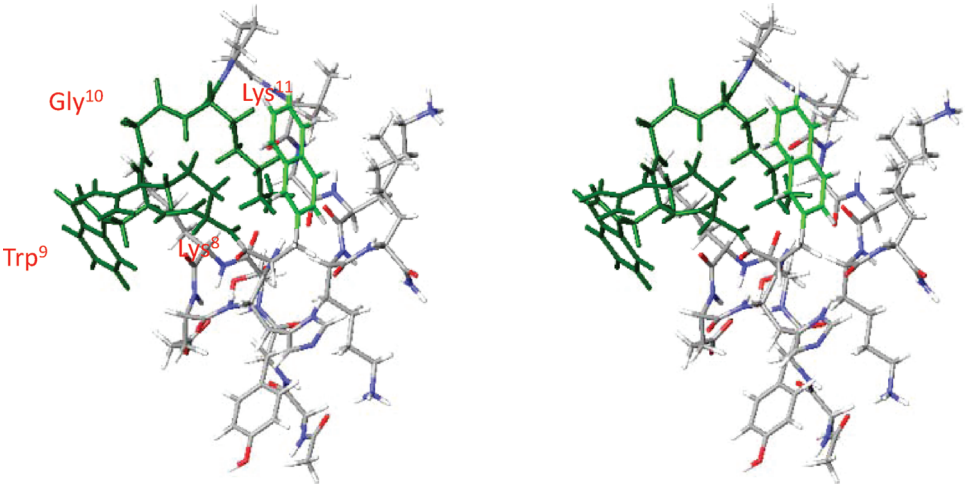

FIGURE 6: Stereoview of N-D-Nal(2′)^7-ACTH1−17. The image was obtained with MCMM/LMCS (Monte Carlo Multiple Minima-Low Frequency Mode)-OPLS 2005 calculations. The new β-turn-like structure (Arg^8-Trp^9-Gly^{10}-Lys^{11}) is colored green.

Table 4: Backbone Torsion Angles (degrees) for the Global Minima of Selected N-D-Nal(2′)^7-ACTH1-17 Analogues[a]

	His^6		D-Phe^7/D-Nal(2′)^7		Arg^8		Trp^9		Gly^{10}/Lys^{10}		Lys^{11}	
	ϕ	ψ	ϕ	ψ	ϕ	ψ	ϕ	ψ	ϕ	ψ	ϕ	ψ
N-D-Nal(2′)^7-ACTH1−17	−144	144	−85	−183	−156	140	−85	131	116	−8	−70	152
MT-II	−108	109	84	0	−122	90	−77	108	−101	103		
SHU9119	−90	49	82	−6	−99	117	−79	111	−90	−68		

[a]This table is based onMCMM/LMCS-OPLS2005 calculations and compared with NMR structures of MTII and SHU9119.

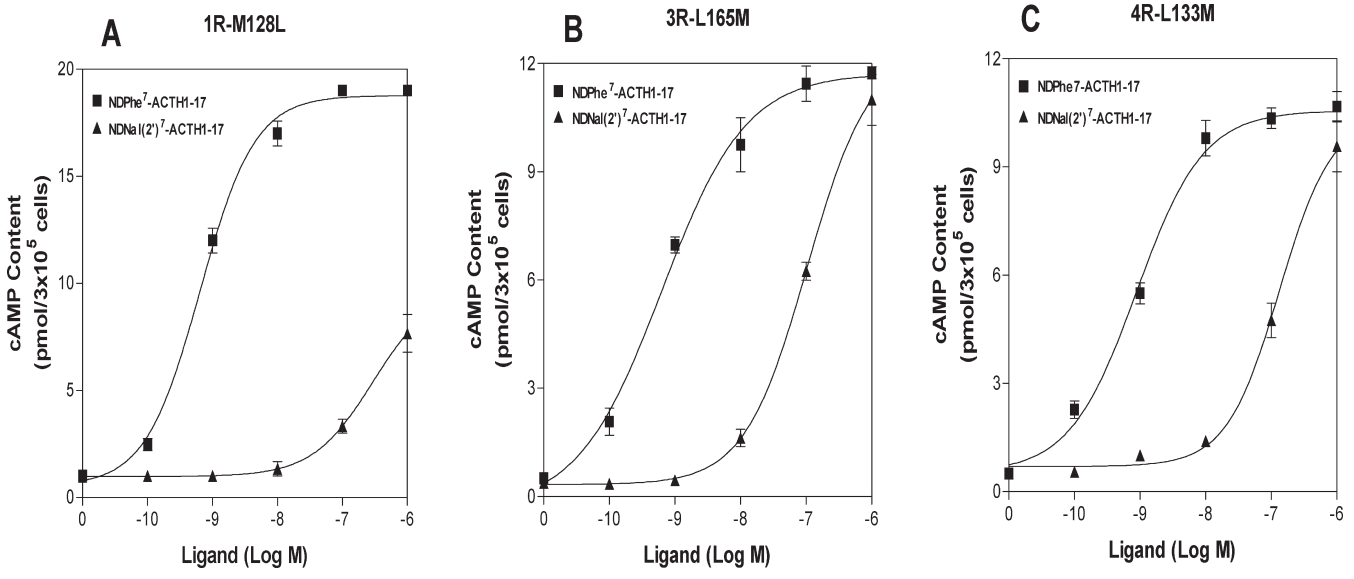

FIGURE 7: Potency of N-D-Nal(2′)^7-ACTH1−17 with the following mutations: M128L in hMC1R, L165M in hMC3R, and L133M in hMC4R. Panel A shows the effects of N-D-Phe^7-ACTH1−17 and N-D-Nal(2′)^7-ACTH1−17 in stimulating cAMP production at the M128L substitution in hMC1R. Panel B shows the effects of D-Phe^7-ACTH1−17 and N-D-Nal(2′)^7-ACTH1−17 in stimulating cAMP production at the L165M substitution in hMC3R. Panel C shows the effects of N-D-Phe^7-ACTH1−17 and N-D-Nal(2′)^7-ACTH1−17 in stimulating cAMP production at the L133M substitution in hMC4R. Data points represent the mean ± standard error of the mean of at least three independent experiments.

C-terminus cause the peptide to fold in a different way which led to the new β-turn, and this β-turn (Arg^8-Trp^9-Gly^{10}-Lys^{11}) brought Trp^9 up as the sole hydrophobic aromatic amino acid that contributes to receptor activation.

Our newly discovered results are consistent with many earlier works published by us and others. Earlier publications have shown the importance of Trp^8 for hMC3R selectivity. D-Trp^8-γ-MSH increases the agonist selectivity at hMC3R. Recently, new evidence also indicates that deletion of Trp^9 of α-MSH allows it to remain an agonist at MC1R but to lose its activity at hMC3R and hMC4R (*49*). Replacement of Arg^8 with a synthetic amino acid leads to selective binding to MC5R and results in a significant decrease in ligand binding affinity and potency at the other MCRs, suggesting that melanocortin receptor subtype

Table 5: Potencies of NDP-α-MSH and N-D-Nal(2′)-ACTH1−17 Analogues at the Mutations in hMC3R, hMC3R, and hMC4R

	EC_{50} (nM)		
	hMC1R-M128L	MC3R-L165M	MC4R-L133M
NDP-α-MSH	0.63 ± 0.1	3.2 ± 0.2	1.9 ± 0.2
D-Phe^7-ACTH1−17	0.71 ± 0.3	3.7 ± 0.1	2.3 ± 0.3
N-D-Nal(2′)^7-ACTH1−17	$>10^3$	78 ± 14	121 ± 11

has different binding sites for different ligands. Further experiments indicate that modification of the Phe residue of NDP-α-MSH resulted in a potent antagonist or partial agonists at MC3R and full, potent agonists at MC4R, suggesting that the molecular mechanism of antagonism at MC3R is different from that at MC4R.

Activation of GPCRs has been proposed to involve the rotation of TM domains with outward movement of their cytoplasmic ends (*50*). This theoretically would enable G-proteins to interact with some of the intracellular loops as well as the C-terminal tail of GPCRs. Some previous MCR studies support this theory since mutations of some TM residues of MCRs can result in inactivation of MCRs (*39*, *40*). A previous finding indicates that the leucine residue in position 165 of hMC3R and position 133 of hMC4R is critical for SHU9119 antagonism. The substitutions of these residues with methionine changed SHU9119 from an antagonist to an agonist (L165M in hMC3R and L133M in hMC4R) (*42*). However, this study indicates that the leucine residues in position 165 of hMC3R and position 133 of hMC4R are not crucial for N-D-Nal(2′)^7-ACTH1−17 activity, supporting the possibility that N-D-Nal(2′)^7-ACTH1−17 has different binding sites at hMC3R and hMC4R compared to N-D-Nal(2′)^7-α-MSH or SHU9119. Amino acid residues Lys^{15}-Lys^{16}-Arg^{17} in N-D-Nal(2′)^7-ACTH1−17 compensate for the loss of the effect of Phe^7 in MSH on receptor activation. However, the corresponding residue in hMC1R (M128) is crucial for N-D-Nal(2′)^7-ACTH1−17 binding and signaling, suggesting that the ligand binding pockets for N-D-Nal(2′)^7-ACTH1−17 at hMC1R, hMC3R, and hMC4R are different.

Finally, we concluded here that N-D-Nal(2′)^7-ACTH1−17 is an agonist at hMC3R and hMC4R; NDP-α-MSH and D-Nal-(2′)^7-ACTH1−17 do not share the same binding site. Arg^8 and Trp^9 in N-D-Nal(2′)^7-ACTH1−17 are critical for hMC3R and hMC4R agonist activity. This provides further evidence of the importance of Trp in hMC3R and hMC4R activity. We have determined that residues Lys^{15}-Lys^{16}-Arg^{17} of N-D-Nal(2′)^7-ACTH1−17 are important for N-D-Nal(2′)^7-ACTH1−17 activity at hMC3R and hMC4R. N-D-Nal(2′)^7-ACTH1−17 has different binding sites at hMC3R and hMC4R compared to that of NDP-α-MSH. This study provides an improved understanding of the fact that the role of the ligand Phe phenyl ring in ACTH activity is different from that of α-MSH. The results from these studies highlight the different receptor activation mechanisms of α-MSH and ACTH and how they may be valuable for future drug design.

REFERENCES

1. Cone, R. D., Lu, D., Koppula, S., Vage, D. I., Klungland, H., Boston, B., Chen, W., Orth, D. N., Pouton, C., and Kesterson, R. A. (1996) The melanocortin receptors: Agonists, antagonists, and the hormonal control of pigmentation. *Recent Prog. Horm. Res. 51*, 287–318.
2. Cone, R. D. (2005) Anatomy and regulation of the central melanocortin system. *Nat. Neurosci. 8*, 571–578.
3. Gispen, W. H., and Isaacson, R. L. (1981) ACTH-induced excessive grooming in the rat. *Pharmacol. Ther. 12*, 209–246.
4. Gantz, I., and Fong, T. M. (2003) The melanocortin system. *Am. J. Physiol. 284*, E468–E474.
5. Chhajlani, V. (1996) Distribution of cDNA for melanocortin receptor subtypes in human tissues. *Biochem. Mol. Biol. Int. 38*, 73–80.
6. Wessells, H., Gralnek, D., Dorr, R., Hruby, V. J., Hadley, M. E., and Levine, N. (2000) Effect of an α-melanocyte stimulating hormone analog on penile erection and sexual desire in men with organic erectile dysfunction. *Urology 56*, 641–646.
7. Li, S. J., Varga, K., Archer, P., Hruby, V. J., Sharma, S. D., Kesterson, R. A., Cone, R. D., and Kunos, G. (1996) Melanocortin antagonists define two distinct pathways of cardiovascular control by α- and γ-melanocyte-stimulating hormones. *J. Neurosci. 16*, 5182–5188.
8. Ni, X. P., Butler, A. A., Cone, R. D., and Humphreys, M. H. (2006) Central receptors mediating the cardiovascular actions of melanocyte stimulating hormones. *J. Hypertens. 24*, 2239–2246.
9. Morgan, C., Thomas, R. E., and Cone, R. D. (2004) Melanocortin-5 receptor deficiency promotes defensive behavior in male mice. *Horm. Behav. 45*, 58–63.
10. Morgan, C., Thomas, R. E., Ma, W., Novotny, M. V., and Cone, R. D. (2004) Melanocortin-5 receptor deficiency reduces a pheromonal signal for aggression in male mice. *Chem. Senses 29*, 111–115.
11. Mogil, J. S., Wilson, S. G., Chesler, E. J., Rankin, A. L., Nemmani, K. V., Lariviere, W. R., Groce, M. K., Wallace, M. R., Kaplan, L., Staud, R., Ness, T. J., Glover, T. L., Stankova, M., Mayorov, A., Hruby, V. J., Grisel, J. E., and Fillingim, R. B. (2003) The melanocortin-1 receptor gene mediates female-specific mechanisms of analgesia in mice and humans. *Proc. Natl. Acad. Sci. U.S.A. 100*, 4867–4872.
12. Vrinten, D. H., Kalkman, C. J., Adan, R. A., and Gispen, W. H. (2001) Neuropathic pain: A possible role for the melanocortin system? *Eur. J. Pharmacol. 429*, 61–69.
13. Lu, D., Willard, D., Patel, I. R., Kadwell, S., Overton, L., Kost, T., Luther, M., Chen, W., Woychik, R. P., and Wilkison, W. O.; et al. (1994) Agouti protein is an antagonist of the melanocyte-stimulating-hormone receptor. *Nature 371*, 799–802.
14. Ollmann, M. M., Wilson, B. D., Yang, Y. K., Kerns, J. A., Chen, Y., Gantz, I., and Barsh, G. S. (1997) Antagonism of central melanocortin receptors in vitro and in vivo by agouti-related protein. *Science 278*, 135–138.
15. Bednarek, M. A., MacNeil, T., Tang, R., Kalyani, R. N., Van der Ploeg, L. H., and Weinberg, D. H. (2001) Potent and selective peptide agonists of α-melanotropin action at human melanocortin receptor 4: Their synthesis and biological evaluation in vitro. *Biochem. Biophys. Res. Commun. 286*, 641–645.
16. Yang, Y. K., Fong, T. M., Dickinson, C. J., Mao, C., Li, J. Y., Tota, M. R., Mosley, R., and Gantz, I. (2000) Molecular determinants of ligand binding to the human melanocortin-4 receptor. *Biochemistry 39*, 14900–14911.
17. Ying, J., Gu, X., Cai, M., Dedek, M., Vagner, J., Trivedi, D. B., and Hruby, V. J. (2006) Design, synthesis, and biological evaluation of new cyclic melanotropin peptide analogues selective for the human melanocortin-4 receptor. *J. Med. Chem. 49*, 6888–6896.
18. Mayer, J. P., Hsiung, H. M., Flora, D. B., Edwards, P., Smith, D. P., Zhang, X. Y., Gadski, R. A., Heiman, M. L., Hertel, J. L., Emmerson, P. J., Husain, S., O'Brien, T, P., Kahl, S. D., Smiley, D. L., Zhang, L., Dimarchi, R. D., and Yan, L. Z. (2005) Discovery of a β-MSH-derived MC-4R selective agonist. *J. Med. Chem. 48*, 3095–3098.
19. Richardson, T. I., Ornstein, P. L., Briner, K., Fisher, M. J., Backer, R. T., Biggers, C. K., Clay, M. P., Emmerson, P. J., Hertel, L. W., Hsiung, H. M., Husain, S., Kahl, S. D., Lee, J. A., Lindstrom, T. D., Martinelli, M. J., Mayer, J. P., Mullaney, J. T., O'Brien, T. P., Pawlak, J. M., Revell, K. D., Shah, J., Zgombick, J. M., Herr, R. J., Melekhov, A., Sampson, P. B., and King, C. H. (2004) Synthesis and structure-activity relationships of novel arylpiperazines as potent and selective agonists of the melanocortin subtype-4 receptor. *J. Med. Chem. 47*, 744–755.
20. Sebhat, I. K., Martin, W. J., Ye, Z., Barakat, K., Mosley, R. T., Johnston, D. B., Bakshi, R., Palucki, B., Weinberg, D. H., MacNeil, T., Kalyani, R. N., Tang, R., Stearns, R. A., Miller, R. R., Tamvakopoulos, C., Strack, A. M., McGowan, E., Cashen, D. E., Drisko, J. E., Hom, G. J., Howard, A. D., MacIntyre, D. E., van der Ploeg, L. H., Patchett, A. A., and Nargund, R. P. (2002) Design and pharmacology of N-[(3R)-1,2,3,4-tetrahydroisoquinolinium-3-ylcarbonyl]-(1R)-1-(4-chlorobenzyl)-2-[4-cyclohexyl-4-(1H-1,2,4-triazol-1-ylmethyl)piperidin-1-yl]-2-oxoethylamine (1), a potent,

selective, melanocortin subtype-4 receptor agonist. *J. Med. Chem. 45*, 4589–4593.
21. Vos, T. J., Caracoti, A., Che, J. L., Dai, M., Farrer, C. A., Forsyth, N. E., Drabic, S. V., Horlick, R. A., Lamppu, D., Yowe, D. L., Balani, S., Li, P., Zeng, H., Joseph, I. B., Rodriguez, L. E., Maguire, M. P., Patane, M. A., and Claiborne, C. F. (2004) Identification of 2-[2-[2-(5-bromo-2-methoxyphenyl)-ethyl]-3-fluorophenyl]-4,5-dihydro-1H-imidazole (ML00253764), a small molecule melanocortin 4 receptor antagonist that effectively reduces tumor-induced weight loss in a mouse model. *J. Med. Chem. 47*, 1602–1604.
22. Hogan, K., Peluso, S., Gould, S., Parsons, I., Ryan, D., Wu, L., and Visiers, I. (2006) Mapping the binding site of melanocortin 4 receptor agonists: A hydrophobic pocket formed by I3.28(125), I3.32(129), and I7.42(291) is critical for receptor activation. *J. Med. Chem. 49*, 911–922.
23. Chen, C., Pontillo, J., Fleck, B. A., Gao, Y., Wen, J., Tran, J. A., Tucci, F. C., Marinkovic, D., Foster, A. C., and Saunders, J. (2004) 4-{(2R)-[3-Aminopropionylamido]-3-(2,4-dichlorophenyl)propionyl}-1-{2-[(2- thienyl)ethylaminomethyl]phenyl}piperazine as a potent and selective melanocortin-4 receptor antagonist: Design, synthesis, and characterization. *J. Med. Chem. 47*, 6821–6830.
24. Hruby, V. J., Cai, M., Cain, J. P., Mayorov, A. V., Dedek, M. M., and Trivedi, D. (2007) Design, synthesis and biological evaluation of ligands selective for the melanocortin-3 receptor. *Curr. Top. Med. Chem. 7*, 1085–1097.
25. Marks, D. L., Hruby, V., Brookhart, G., and Cone, R. D. (2006) The regulation of food intake by selective stimulation of the type 3 melanocortin receptor (MC3R). *Peptides 27*, 259–264.
26. King, S. H., Mayorov, A. V., Balse-Srinivasan, P., Hruby, V. J., Vanderah, T. W., and Wessells, H. (2007) Melanocortin receptors, melanotropic peptides and penile erection. *Curr. Top. Med. Chem. 7*, 1098–1106.
27. Cai, M., Mayorov, A. V., Ying, J., Stankova, M., Trivedi, D., Cabello, C., and Hruby, V. J. (2005) Design of novel melanotropin agonists and antagonists with high potency and selectivity for human melanocortin receptors. *Peptides 26*, 1481–1485.
28. Hruby, V. J., Lu, D., Sharma, S. D., Castrucci, A. L., Kesterson, R. A., al-Obeidi, F. A., Hadley, M. E., and Cone, R. D. (1995) Cyclic lactam α-melanotropin analogues of Ac-Nle4-cyclo[Asp5,D-Phe7, Lys10] α-melanocyte-stimulating hormone-(4−10)-NH2 with bulky aromatic amino acids at position 7 show high antagonist potency and selectivity at specific melanocortin receptors. *J. Med. Chem. 38*, 3454–3461.
29. Vergoni, A. V., Poggioli, R., Marrama, D., and Bertolini, A. (1990) Inhibition of feeding by ACTH-(1−24): Behavioral and pharmacological aspects. *Eur. J. Pharmacol. 179*, 347–355.
30. Grieco, P., Balse, P. M., Weinberg, D., MacNeil, T., and Hruby, V. J. (2000) D-Amino acid scan of γ-melanocyte-stimulating hormone: Importance of Trp(8) on human MC3 receptor selectivity. *J. Med. Chem. 43*, 4998–5002.
31. Cai, M., Mayorov, A. V., Cabello, C., Stankova, M., Trivedi, D., and Hruby, V. J. (2005) Novel 3D pharmacophore of α-MSH/γ-MSH hybrids leads to selective human MC1R and MC3R analogues. *J. Med. Chem. 48*, 1839–1848.
32. Balse-Srinivasan, P., Grieco, P., Cai, M., Trivedi, D., and Hruby, V. J. (2003) Structure-activity relationships of γ-MSH analogues at the human melanocortin MC3, MC4, and MC5 receptors. Discovery of highly selective hMC3R, hMC4R, and hMC5R analogues. *J. Med. Chem. 46*, 4965–4973.
33. Mayorov, A. V., Cai, M., Chandler, K. B., Petrov, R. R., Van Scoy, A. R., Yu, Z., Tanaka, D. K., Trivedi, D., and Hruby, V. J. (2006) Development of cyclic γ-MSH analogues with selective hMC3R agonist and hMC3R/hMC5R antagonist activities. *J. Med. Chem. 49*, 1946–1952.
34. Kavarana, M. J., Trivedi, D., Cai, M., Ying, J., Hammer, M., Cabello, C., Grieco, P., Han, G., and Hruby, V. J. (2002) Novel cyclic templates of α-MSH give highly selective and potent antagonists/agonists for human melanocortin-3/4 receptors. *J. Med. Chem. 45*, 2644–2650.
35. Grieco, P., Lavecchia, A., Cai, M., Trivedi, D., Weinberg, D., MacNeil, T., Van der Ploeg, L. H., and Hruby, V. J. (2002) Structure-activity studies of the melanocortin peptides: Discovery of potent and selective affinity antagonists for the hMC3 and hMC4 receptors. *J. Med. Chem. 45*, 5287–5294.
36. Balse-Srinivasan, P., Grieco, P., Cai, M., Trivedi, D., and Hruby, V. J. (2003) Structure-activity relationships of novel cyclic α-MSH/β-MSH hybrid analogues that lead to potent and selective ligands for the human MC3R and human MC5R. *J. Med. Chem. 46*, 3728–3733.
37. Gantz, I., Miwa, H., Konda, Y., Shimoto, Y., Tashiro, T., Watson, S. J., DelValle, J., and Yamada, T. (1993) Molecular cloning, expression, and gene localization of a fourth melanocortin receptor. *J. Biol. Chem. 268*, 15174–15179.
38. Mountjoy, K. G., Robbins, L. S., Mortrud, M. T., and Cone, R. D. (1992) The cloning of a family of genes that encode the melanocortin receptors. *Science 257*, 1248–1251.
39. Chen, M., Aprahamian, C. J., Celik, A., Georgeson, K. E., Garvey, W. T., Harmon, C. M., and Yang, Y. (2006) Molecular characterization of human melanocortin-3 receptor ligand-receptor interaction. *Biochemistry 45*, 1128–1137.
40. Chen, M., Georgeson, K. E., Harmon, C. M., Haskell-Luevano, C., and Yang, Y. (2006) Functional characterization of the modified melanocortin peptides responsible for ligand selectivity at the human melanocortin receptors. *Peptides 27*, 2836–2845.
41. Chen, M., Cai, M., Aprahamian, C. J., Georgeson, K. E., Hruby, V., Harmon, C. M., and Yang, Y. (2007) Contribution of the conserved amino acids of the melanocortin-4 receptor in [corrected] [Nle4, D-Phe7]-α-melanocyte-stimulating [corrected] hormone binding and signaling. *J. Biol. Chem. 282*, 21712–21719.
42. Yang, Y., Chen, M., Lai, Y., Gantz, I., Georgeson, K. E., and Harmon, C. M. (2002) Molecular determinants of human melanocortin-4 receptor responsible for antagonist SHU9119 selective activity. *J. Biol. Chem. 277*, 20328–20335.
43. Haskell-Luevano, C., Cone, R. D., Monck, E. K., and Wan, Y. P. (2001) Structure activity studies of the melanocortin-4 receptor by in vitro mutagenesis: Identification of agouti-related protein (AGRP), melanocortin agonist and synthetic peptide antagonist interaction determinants. *Biochemistry 40*, 6164–6179.
44. Sawyer, T. K., Sanfilippo, P. J., Hruby, V. J., Engel, M. H., Heward, C. B., Burnett, J. B., and Hadley, M. E. (1980) 4-Norleucine, 7-D-phenylalanine-α-melanocyte-stimulating hormone: A highly potent α-melanotropin with ultralong biological activity. *Proc. Natl. Acad. Sci. U.S.A. 77*, 5754–5758.
45. DeBlasi, A., O'Reilly, K., and Motulsky, H. J. (1989) Calculating receptor number from binding experiments using same compound as radioligand and competitor. *Trends Pharmacol. Sci. 10*, 227–229.
46. Yang, Y. K., Ollmann, M. M., Wilson, B. D., Dickinson, C., Yamada, T., Barsh, G. S., and Gantz, I. (1997) Effects of recombinant agouti-signaling protein on melanocortin action. *Mol. Endocrinol. 11*, 274–280.
47. Mizoue, L. S., Bazan, J. F., Johnson, E. C., and Handel, T. M. (1999) Solution structure and dynamics of the CX3C chemokine domain of fractalkine and its interaction with an N-terminal fragment of CX3CR1. *Biochemistry 38*, 1402–1414.
48. István Kolossváry, W. C. G. (1999) Low-mode conformational search elucidated: Application to C39H80 and flexible docking of 9-deazaguanine inhibitors into PNP. *J. Comput. Chem. 20*, 1671–1684.
49. Bednarek, M. A., Macneil, T., Tang, R., Fong, T. M., Angeles Cabello, M., Maroto, M., and Teran, A. (2008) Analogs of α-melanocyte stimulating hormone with high agonist potency and selectivity at human melanocortin receptor 1b: The role of Trp(9) in molecular recognition. *Biopolymers 89*, 401–408.
50. Gether, U. (2000) Uncovering molecular mechanisms involved in activation of G protein-coupled receptors. *Endocr. Rev. 21*, 90–113.